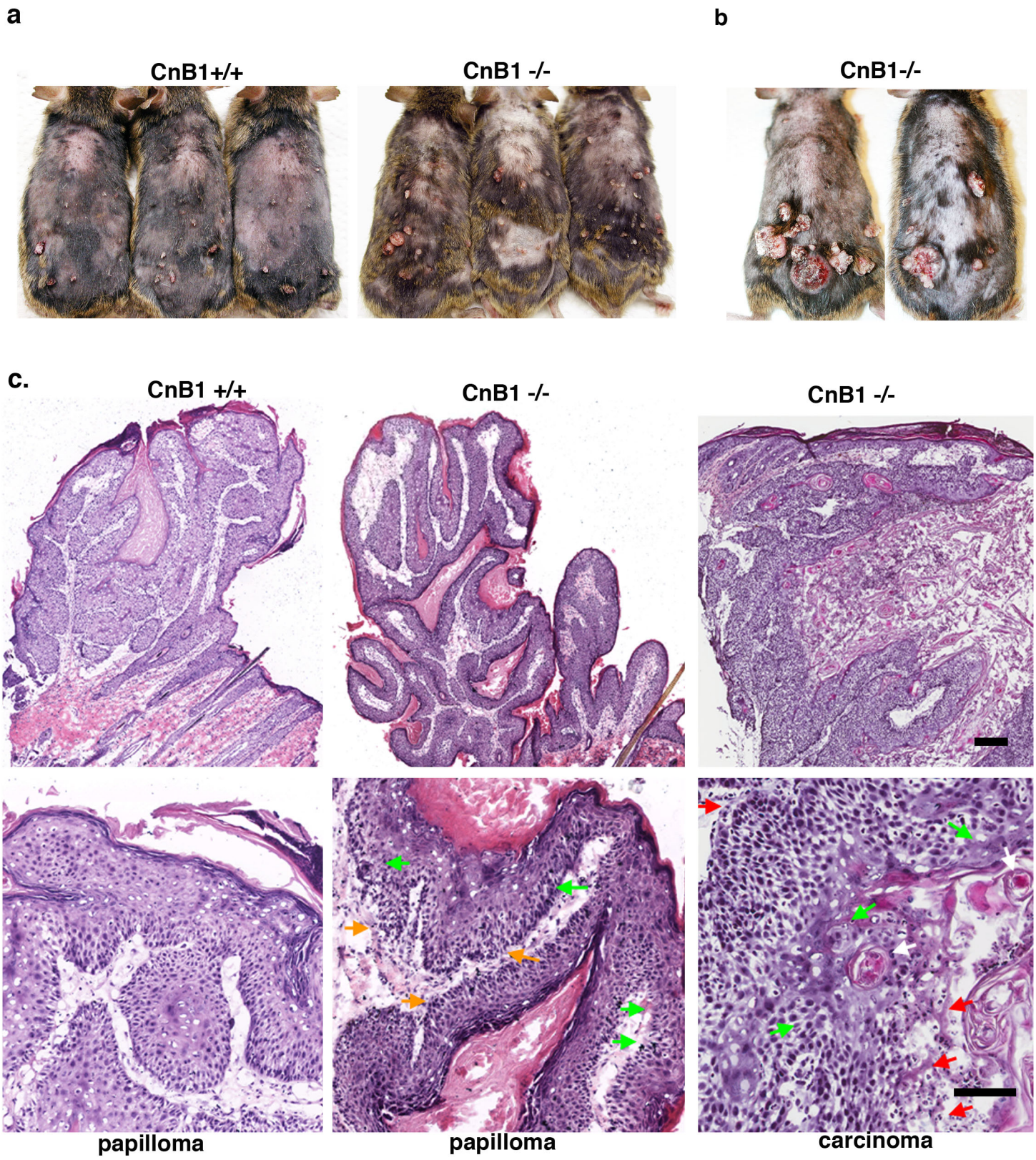

Wu et al_Suppl.Fig. 1

Supplemental Figure 1. Keratinocyte-specific deletion of the CnB1 gene results in increased susceptibility to chemically-induced skin carcinogenesis

a, photographs of 3 mice with a keratinocyte-specific deletion of the CnB1 gene (CnB1 -/-) in parallel with controls with an intact CnB1 gene (CnB1+/+), at 3 months after initiation of the multistep carcinogenesis protocol (via topical DMBA / TPA treatment, as described in the methods section). Note the larger number of papillomas, of larger size, in mice with the CnB1 gene relative to the controls, quantified in Fig. 1a. **b,** photographs of two other mice with the CnB1 deletion with large papillomas in the process of malignant conversion at 5 months after initiation, as indicated macroscopically by an infiltrating solid base and as confirmed histologically as shown below. **c,** histological analysis of tumours from CnB1+/+ versus CnB1 -/- mice. Left and middle panels: low and high magnification images representative of 8 independent papillomas per genotype. Control mice developed exophytic papilloma with regular acanthosis and compact keratinization, preserving cytological regularity and clear demarcation towards the dermis. By contrast, papillomas of mice with the CnB1 deletion showed irregular acanthosis and keratinization of the epithelium, with nests of heterogeneous keratinocytes (green arrows) and incipient breach of the dermal-epidermal junction (orange arrows). Right panels : low and high magnification images of malignant tumour progression in mice with the CnB1 deletion. Images illustrate a squamous cell carcinoma of the skin with pronounced cellular atypia (green arrows), foci of ectopic keratinization (white arrows) as well as invasive growth into the surrounding tissue (red arrows). Bars: 50μm

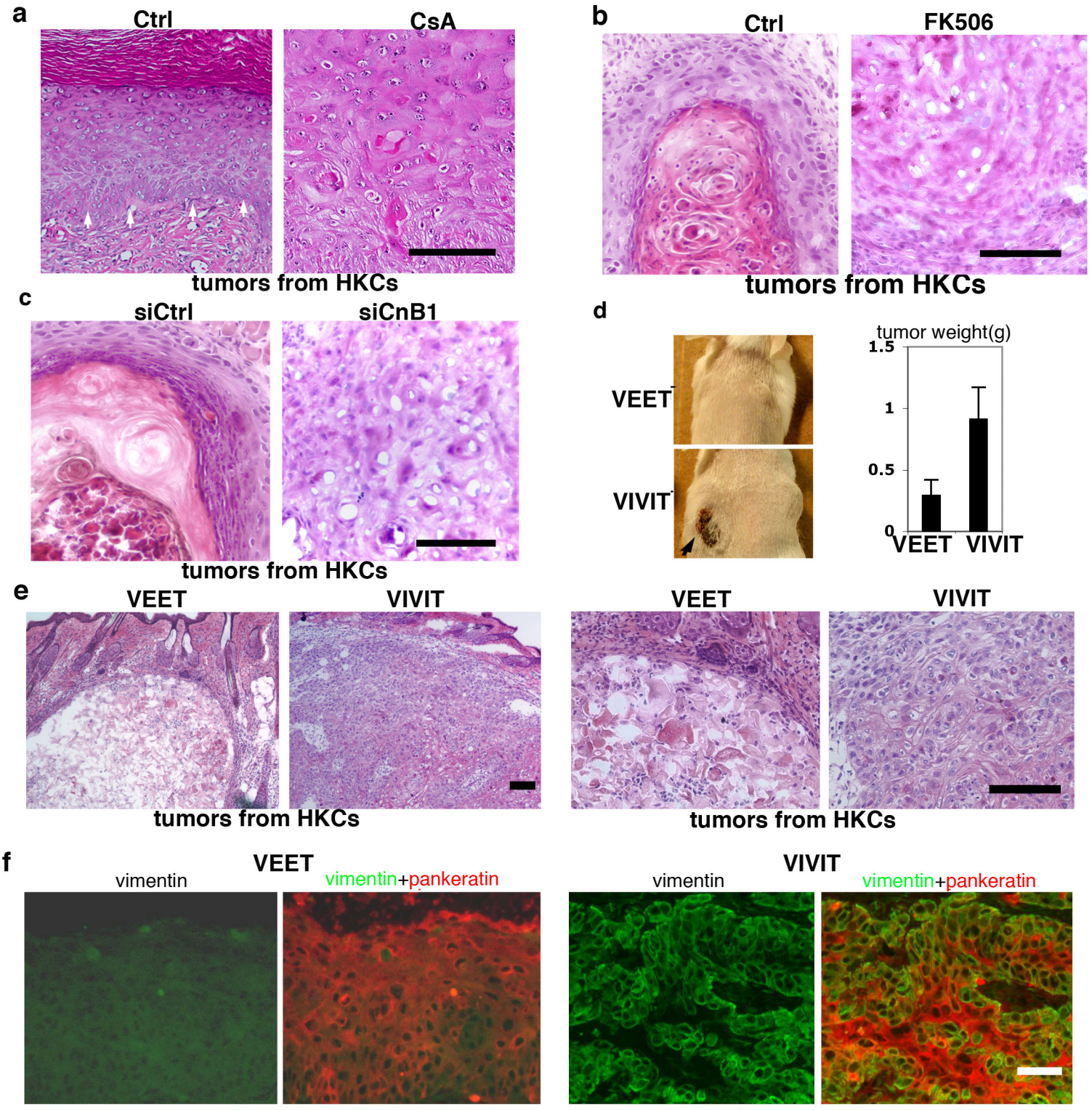

Wu et al_Suppl.Fig.2

Supplemental Figure 2. Calcineurin/NFAT inhibition promotes tumourigenesis by oncogenic *ras* expressing primary keratinocytes

a, High magnification histological images of tumours formed by H-*ras*^{V12} expressing HKCs grafted onto Scid mice plus/minus CsA treatment. Experimentally, HKCs infected with a H-*ras*^{V12} transducing retrovirus (LZRS-ras^{V12})[1] were grafted onto the back of immunocompromised (Scid) mice, followed by treatment, every other day, with CsA (via injection into the transplantation chamber, 20 μg/g body weight) or ethanol vehicle alone (4 mice per group). 8 weeks later, grafted tissues were retrieved for histological analysis and average weight determination (as shown in Fig. 1b). H-*ras*^{V12}-expressing keratinocytes in control mice gave rise to an acanthotic epithelium well separated from the underlying dermal tissues. By contrast, the same cells in the CsA-treated animals produced invasive lesions with histological features of cutaneous SCC (grade II-III), with a disordered pattern of growth and large cells with nuclear atypia and little or no signs of keratinization. Photographs are representative of the histological differences found in all cases. Bar = 100 μm. **b-c,** High magnification images of the lesions formed by H-*ras*^{V12} expressing HKCs in mice treated with FK506 (b) or cells transfected with siRNA for CnB1 (**c**). HKCs infected with a H-*ras*^{V12} transducing retrovirus as in **a,** were injected at the dermal-epidermal junction of immunocompromised (Scid) mice utilizing a technique previously used for hair follicle reconstitution assays[2] (10^6 cells per injection, two side flank injections per mouse). Mice were subsequently treated with CsA (by I.P. injection; 20 μg/g body weight in ethanol) or FK506 (2 μg/g body weight in DMSO) and corresponding vehicle control every other day. As an alternative approach, HKCs were transfected with siRNAs against the CnB1 gene (siCnB1) or scrambled siRNA controls (siCtrl) prior to infection with the H-*ras*^{V12} transducing retrovirus and injection into mice. >80% efficiency of siRNA-mediated CnB1

knockdown was verified by immunoblot and real time RT-PCR analysis as shown in Fig. 2b and Suppl. Fig. 8b. In all cases, mice were sacrificed at 10 days after cell injections and the nodules found at the site of injections processed for histological analysis. Histological images are representative of differences found in all cases, as summarized in Fig. 1c. Bar = 100 μm. **d,** H-*ras*^{V12} expressing HKCs were injected at the dermal-epidermal junction of Scid mice followed by treatment with the VIVIT or control VEET peptides (by I.P. injection; 10 μg/g body weight in ethanol). Mice were sacrificed 6 weeks later. Pronounced tumour formation was already evident by macroscopic inspection of the VIVIT-treated mice, together with overlying skin ulcerations (lower left panel, black arrow). A set of 5 tumours from VIVIT- versus VEET- treated mice were separated from surrounding tissue for average weight determination (right panel). **e**, Tumours from the above experiment were processed for histological analysis, with left and right panels corresponding to low and high magnification images, respectively. In all cases, H-*ras*^{V12}-expressing keratinocytes in control VEET-treated mice gave rise to highly keratinized cysts with limited surrounding cellularity. By contrast, the same cells in the VIVIT-treated animals produced invasive lesions with histological features of cutaneous SCC, with little or no signs of keratinization. Bars: 50μm. **f,** Lesions formed by H-*ras*^{V12} expressing HKCs in VIVIT and VEET-treated animals as in the previous panels were analysed by double immuno-fluorescence with antibodies against pankeratin (red) and vimentin (green) as indicated. The anti-vimentin antibodies are human specific, do not cross-react with mouse tissue and were used in combination with the pankeratin antibodies to distinguish tumour cells of human origin from mouse tissues. Bar = 25 μm.

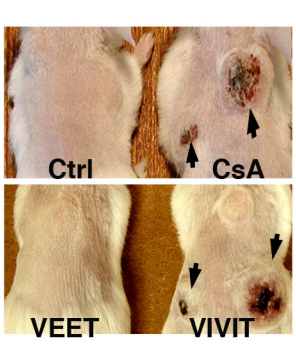

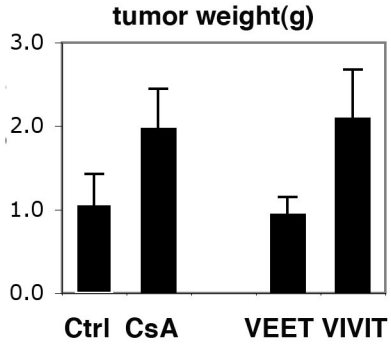

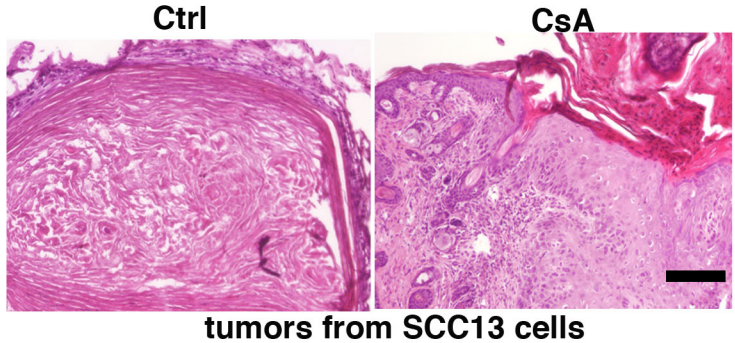

tumors from SCC13 cells

Wu et al_Suppl. Fig.3

Supplemental Figure 3. Calcineurin/NFAT inhibition promotes tumourigenesis of keratinocyte-derived SCC cells.

SCC13 cells were injected at the dermal-epidermal junction of immunocompromised (Scid) mice followed by treatment with either CsA or the VIVIT peptide[3] in parallel with corresponding controls, and sacrificed 6 weeks later. Pronounced tumour formation was already evident by macroscopic inspection of the CsA- and VIVIT-treated mice, together with overlying skin ulcerations (left panels, black arrows). A set of 5 tumours per condition was separated from surrounding tissue for average weight determination (middle panels). Histological images are representative of lesions formed by SCC13 cells in control versus CsA-treated mice (right panels) with similar differences being found in mice treated with VIVIT versus control VEET peptide. Bar = 100 μm.

a

quantification of histological lesions

conditions	well differentiated cysts	highly cellular lesions
SCC13+siCtrl	4/5	0/5
SCC13+sip53	1/5	4/5

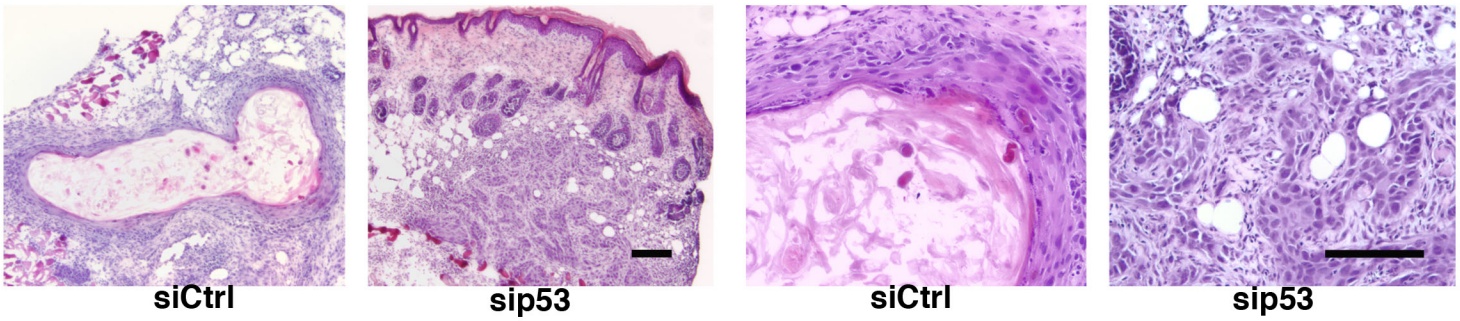

b

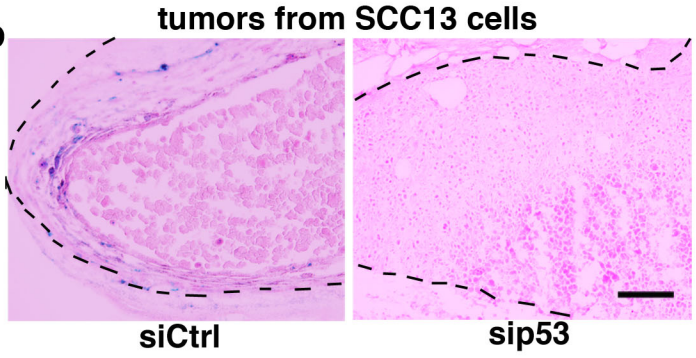

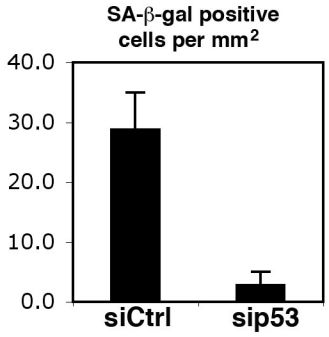

c

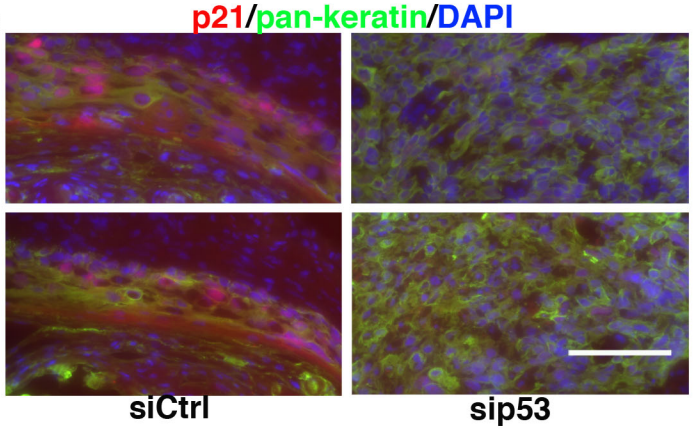

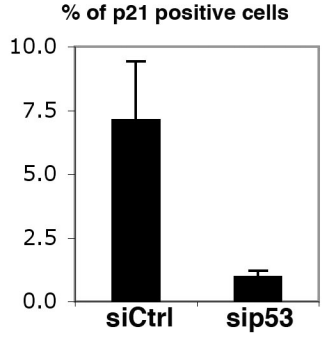

WU et al_ Suppl.Fig.4

Supplemental Figure 4. Knockdown of p53 in SCC cells promotes tumourigenesis and suppresses senescence.

a, SCC13 cells were transfected with p53-specific siRNA (sip53) or scramble siRNA control (sictrl), and, 12 hours later, injected at the dermal-epidermal junction of immunocompromised (Scid) mice. Preliminary experiments showed >80% knockdown of p53 expression as also previously demonstrated [4]. As summarized in the upper panel and shown in the low and high magnification images below, control SCC13 cells formed highly keratinized cysts, while cells with knockdown of p53 produced lesions with histological features of poorly to moderately differentiated SCC. bars=100 μm. **b,** Tissue sections of lesions formed by SCC13 cells plus/minus p53 knockdown (from the experiment in panel a) were stained for SA-β-galactosidase activity (left panels) with the quantification of SA-β-gal positive cells shown on the right. Bar=100μm. **c,** Tissue sections of lesions formed by SCC13 cells plus/minus p53 knockdown were analyzed by immunofluorescence with antibodies against $p21^{WAF1/Cip1}$ (red) and pankeratin (green; for injected keratinocyte identification), with DAPI nuclear staining (Blue). Two different images per conditions are shown together with a quantification (on the right) of the percentage of pan-keratin positive cells that were positive for p21 expression. Bar=100μm

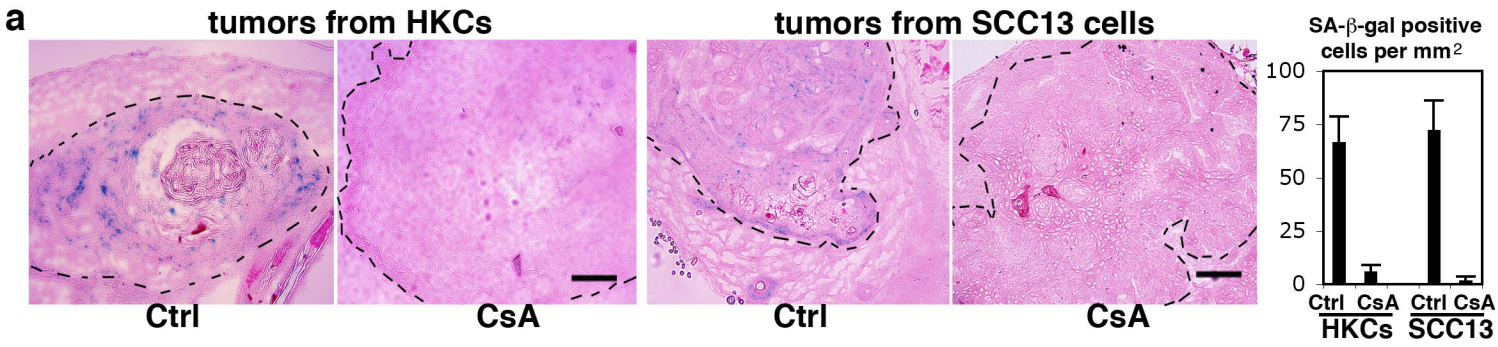

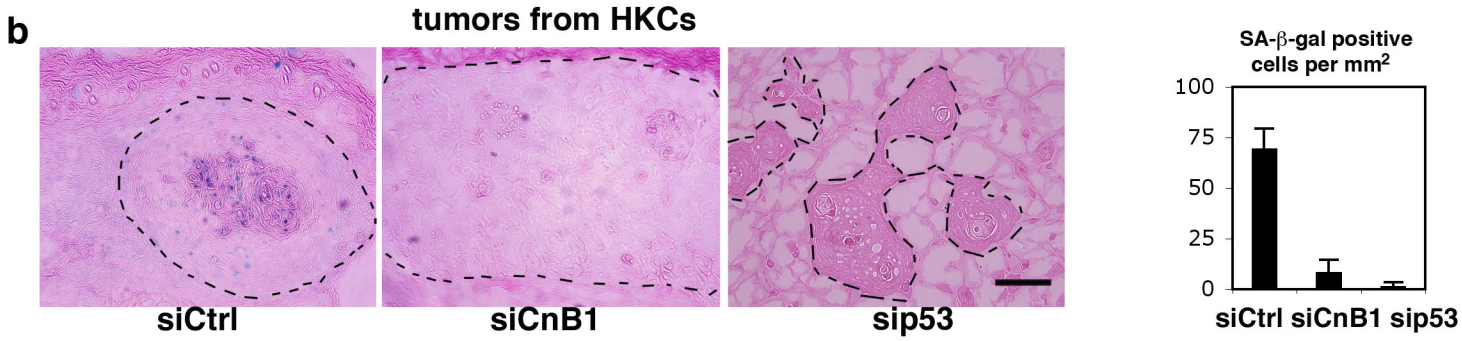

WU et al_ Suppl.Fig.5

Supplemental Figure 5. Calcineurin/NFAT inhibition promotes cancer cell tumourigenesis and suppresses senescence

a, low magnification images of the same sections stained for senescence-associated ß-galactosidase activity (SA-ß-gal) in Fig. 1d. Endogenous ß-galactosidase activity at suboptimal pH (pH 6) is thought to reflect increased lysosomal activity that occurs in senescent cells[5]. Parallel activity assays at optimal pH (pH 4) were performed as control for ß-galactosidase activity in cells, irrespective of their growing or senescent state. SA-ß-Gal activity yielded a blue colour, while eosin was used for counter staining (red). Images are representative of several independent fields and a minimum of two lesions per condition. The numbers of SA-ß-gal positive cells per mm^2 of solid tumour areas (delimited by dotted lines) are given in the right panel. Bar=50μm. **b,** low magnification images of the same SA-ß-gal stained sections shown in Fig. 1e, plus quantification of SA-ß-gal positive cells counted as in the previous panel. Bar=50μm.

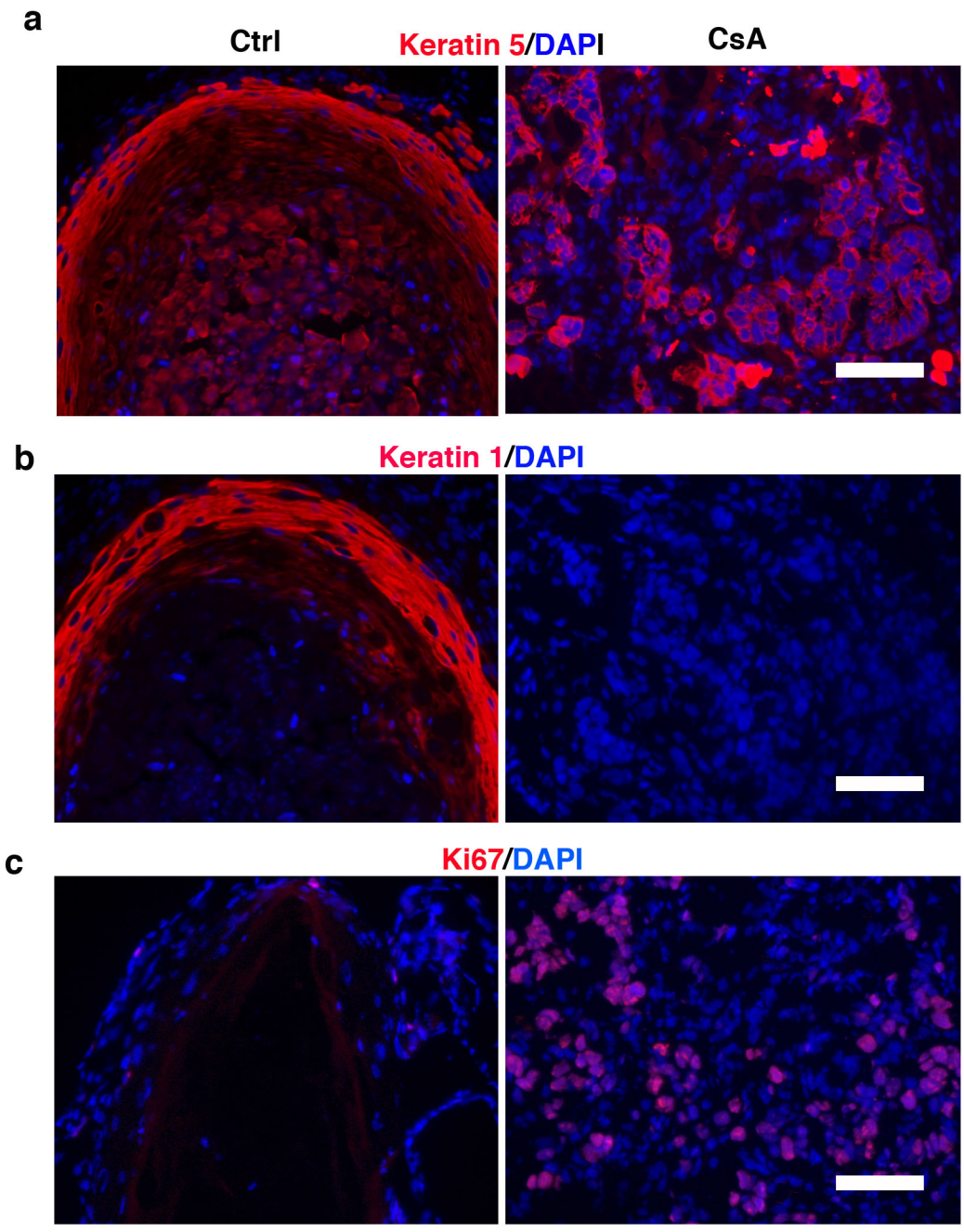

Wu et al_Suppl. Fig.6

Supplemental Figure 6. Calcineurin/NFAT inhibition results in increased tumour cell proliferation and hampered differentiation

a-c, Tissue sections of the lesions formed by H-*ras*^{V12} expressing HKCs in CsA-treated mice versus controls (Ctrl) from the experiment of Fig. 1c, were analyzed by immunofluorescence with antibodies against Ki67 and Keratin 1, as markers of cell proliferation and differentiation, respectively, and Keratin 5, for keratinocyte identification. DAPI was utilized for nuclear counterstaining. Images are representative of several independent fields and a minimum of two lesions per condition. Bars = 50 μm

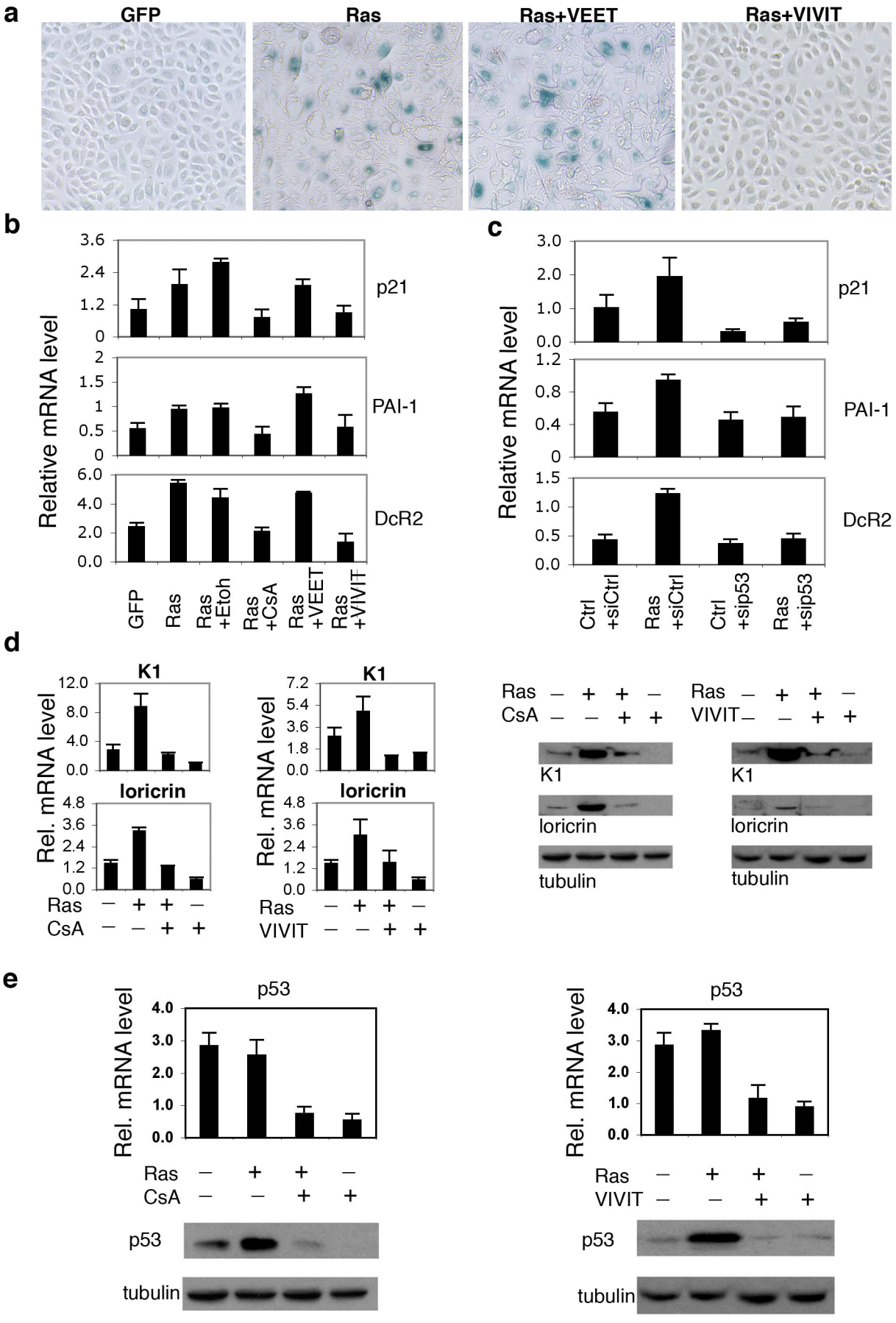

Wu et al_Suppl. Fig. 7

Supplemental Figure 7. Calcineurin/NFAT inhibition overcomes oncogene-induced senescence and suppresses p53 expression.

a, HKCs were infected with a H-*ras*^{V12} expressing retrovirus (Ras) versus GFP expressing control (GFP) followed (3 hours after infection) by treatment with VIVIT or control VEET peptide (2 μM) for 48 hours. Cells were analyzed by *in situ* chromogenic assay for senescence-associated ß-galactosidase activity (SA-ß-Gal). **b,** HKCs were infected with control and H-*ras*^{V12} expressing retroviruses, followed (3 hours after infection) by treatment with CsA (5 μM in ethanol) or ethanol vehicle alone (Etoh), or with VIVIT and control VEET peptide (2 μM) for 24 hours. Cells were analyzed for expression of the indicated genes by real time RT-PCR utilizing 34B4 for normalization. **c,** HKCs were transfected with siRNAs against p53 or scrambled siRNA controls under conditions that result in >80% p53 knock down. 48 hours after transfection, cells were infected with GFP control and H-*ras*^{V12} expressing retroviruses, followed 24 hours later, by analysis of the indicated genes by real time RT-PCR, with 36B4 for normalization. **d,** HKCs infected with the GFP control or H-*ras*^{V12} expressing retroviruses were treated with CsA or VIVIT in parallel with the corresponding controls as in the previous panels. Expression of the Keratin1 (K1) and loricrin differentiation markers was assessed by real time RT-PCR analysis and immunoblotting (left and right panels, respectively). **e,** Same samples as in the previous panel were analyzed for levels of p53 expression by real time RT-PCR and immunoblotting as indicated.

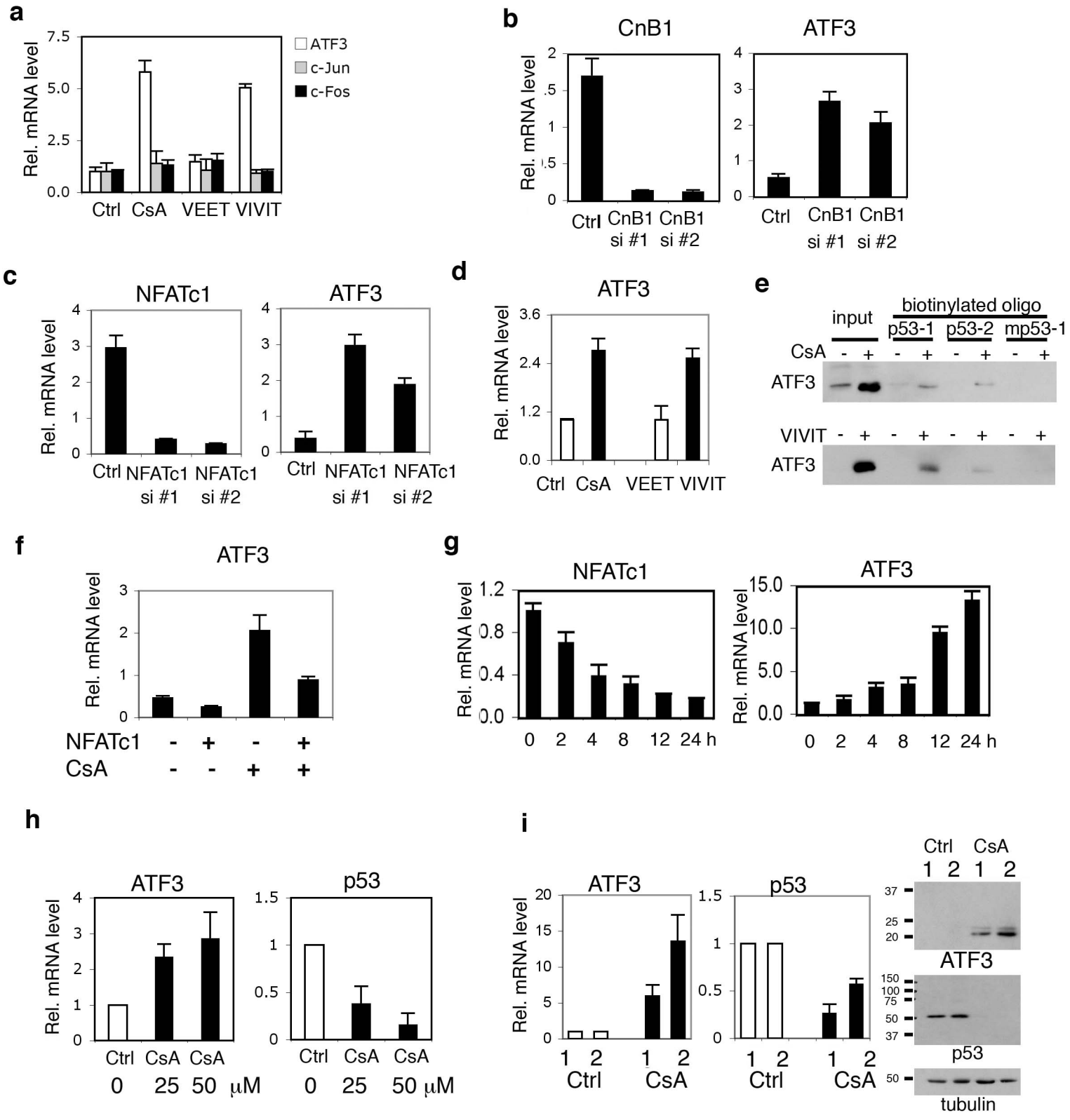

Wu et al_Suppl. Fig.8

Supplemental Figure 8. Calcineurin/NFAT inhibition causes a parallel increase of ATF3 expression and down-modulation of p53

a, HKCs were treated with either CsA (5 μM) or VIVIT (2 μM) and corresponding controls for 24 hours, followed by real time RT-PCR analysis of ATF3, c-Jun and c-Fos mRNA expression, using 36B4 for normalization, with similar results being obtained after normalization for β-actin mRNA. **b-c,** HKCs were transfected with two sets of siRNAs specific for the calcineurin B1 (CnB1) (**b**) or NFATc1 (**c**) genes, in parallel with scrambled siRNA controls (Ctrl). 96 hours after transfection, cells were analyzed by real time RT-PCR analysis for CnB1, NFATc1 and ATF3 expression. **d,** SCC13 cells were treated with either CsA or VIVIT in parallel with corresponding controls, followed by analysis of ATF3 expression by real time RT-PCR, as in the experiment of (a). **e,** HKCs were treated with either CsA or VIVIT in parallel with corresponding controls for 24 hours. Cell lysates were incubated with two biotinylated oligonucleotide sequences of the p53 promoter containing fully conserved ATF3 binding sites (p53-1 and p53-2, corresponding, respectively, to nucleotide positions -420 to -358 and -2105 to -2039 from the initiation codon) in parallel with a mutated oligonucleotide of the first sequence (mp53-1), with internal nucleotide substitutions disrupting the ATF3 binding site. DNA-bound proteins were precipitated by streptavidin-agarose, and recovered ATF3 was detected by immunoblotting. **f,** HKCs were infected with a retrovirus expressing a constitutively active form of NFATc1 (+)[6] or GFP expressing control (-) followed, 48 hours after infection, by CsA treatment for 24 hours. ATF3 expression was assessed by real time RT-PCR, with immunoblot results shown in Fig. 2c. **g,** HKCs were transfected with siRNAs specific for the NFATc1 gene in parallel with scrambled siRNA controls, followed by a time course determination of levels of endogenous NFATc1 versus ATF3 expression, via real time RT-PCR. **h,** Freshly excised human

skin samples were placed in semisolid medium and treated with CsA at the indicated concentrations or ethanol control (black and white bars, respectively) for 48 hours. The epidermis was separated from the underlying dermis by a brief heat treatment followed by total RNA preparation and analysis of mRNA expression of the ATF3 and p53 genes by real time RT-PCR, using 36B4 mRNA for normalization. **i,** Total RNA was extracted from tumours formed by H-*ras*^{V12} expressing HKCs in Scid mice plus/minus treatment with CsA, as shown in Fig. 1b, followed by real time RT-PCR analysis for ATF3 and p53 expression, using 36B4 for normalization (left panels). Protein extracts of tumours from control versus CsA-treated mice were also analyzed by immunoblotting with the indicated proteins (right panels). The position of the molecular weight size markers (in kD) is indicated.

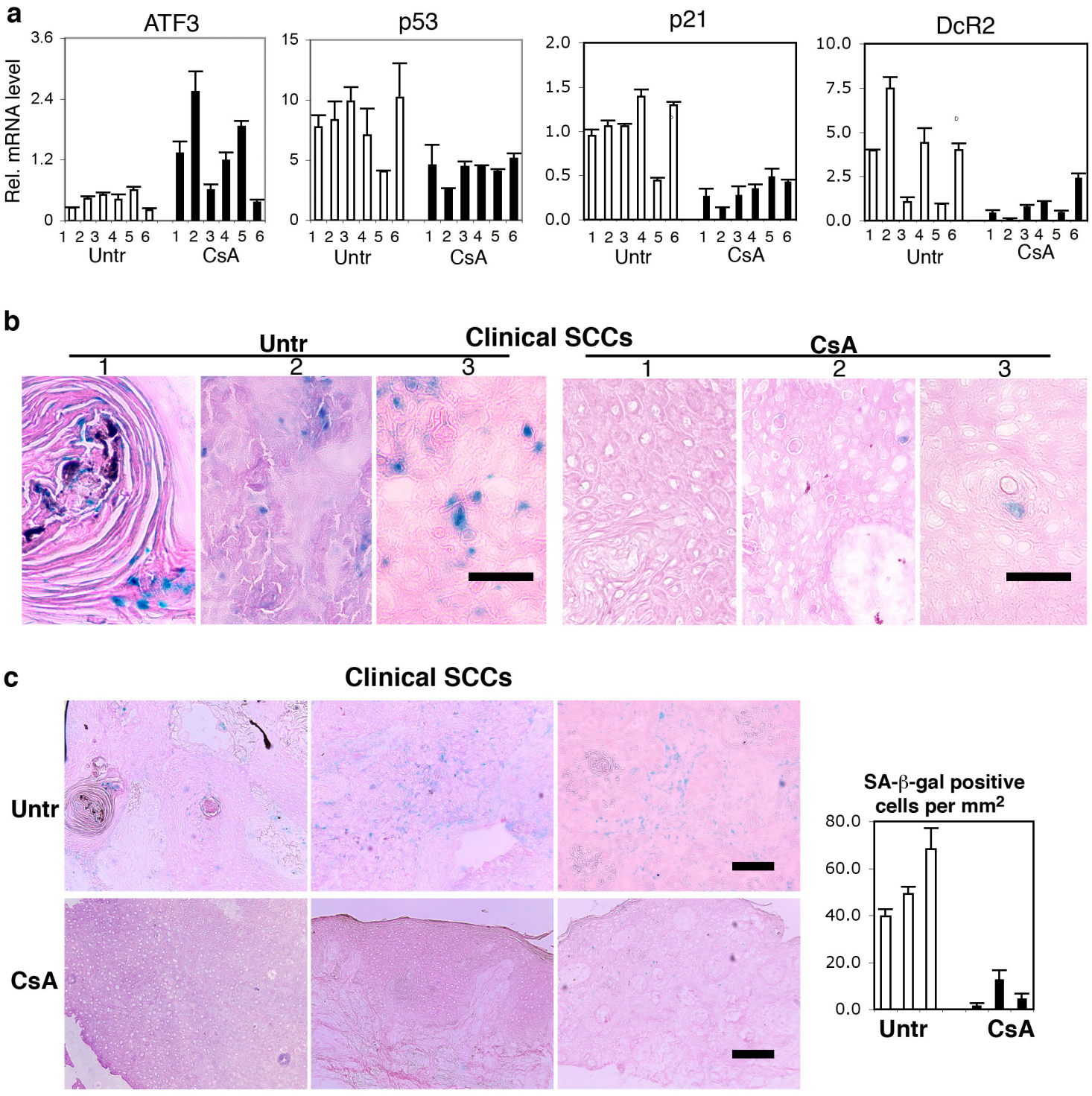

Wu et al_Suppl. Fig. 9

Supplemental Figure 9. Suppression of senescence in SCCs of patients under CsA treatment

a, Total RNA was extracted from SCCs from 6 patients under CsA treatment (CsA) in parallel with SCCs from site and age-matched untreated patients (Untr), followed by real time RT-PCR analysis for the ATF3, p53 and senescence marker genes: $p21^{WAF1/Cip1}$ DcR2, using 36B4 for normalization. **b,** Tissue sections of SCCs from 3 patients under CsA treatment (CsA) were analyzed in parallel with SCCs from the untreated general population (Untr) for SA-β-galactosidase activity (blue), using eosin (red) for counter staining. Images are representative of several independent fields per tumour. Bars: 50μm. **c,** low magnification images of the sections shown in the previous panel, together with a quantification, on the right, of number of SA-β-gal positive cells. Bars: 100μm.

a

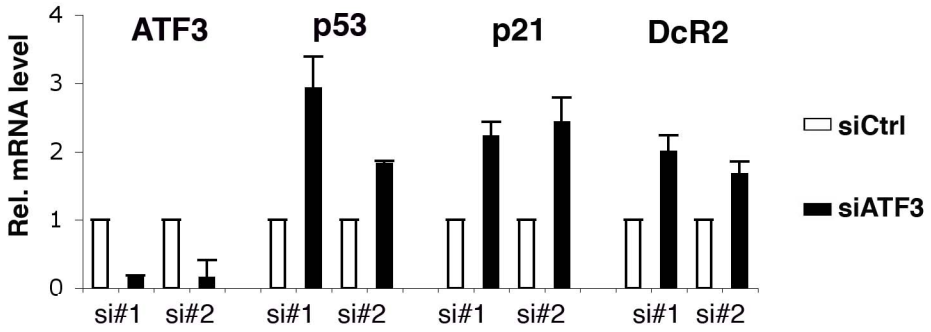

b

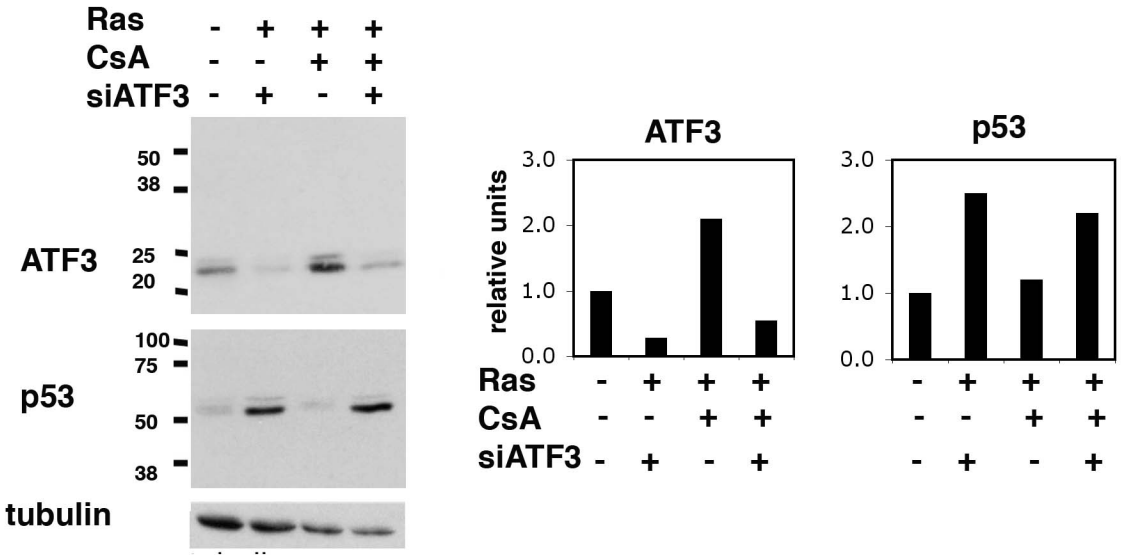

Wu et al_Suppl. Fig. 10

Supplemental Figure 10. ATF3 knockdown results in up-regulation of p53 and p53-dependent senescence genes.

a, HKCs were transfected with two siRNAs specific for ATF3 in parallel with scrambled controls (#1 and 2, black and white bars, respectively), followed, 48 hours later, by real time RT-PCR analysis of ATF3, p53, p21 and DcR2 gene expression. **b,** Larger images of the immunoblots shown in Fig. 3d, with the position of size markers (in kD) indicated. The results were quantified by densitometric scanning of the autoradiographs (right panels), with p53 and ATF3 protein levels being expressed in arbitrary values relative to the control, after internal normalization for γ-tubulin expression.

a

Quantification of histological lesions

conditions	well differentiated cysts	highly cellular lesions
HKCs+Ctrl	5/6	0/6
HKCs+ATF3	1/6	4/6

b

Quantification of histological lesions

conditions	well differentiated cysts	highly cellular lesions
scc13+Ctrl	5/6	1/6
scc13+ATF3	1/6	5/6
scc12+Ctrl	4/6	1/6
scc12+ ATF3	0/6	5/6

c

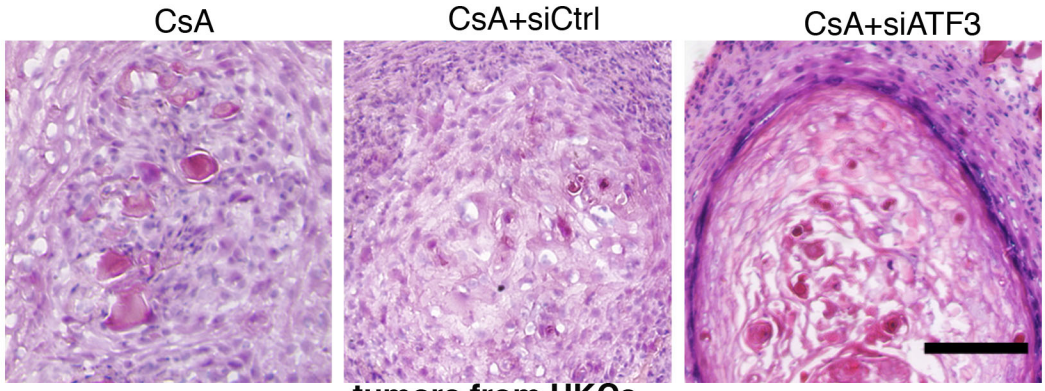

d

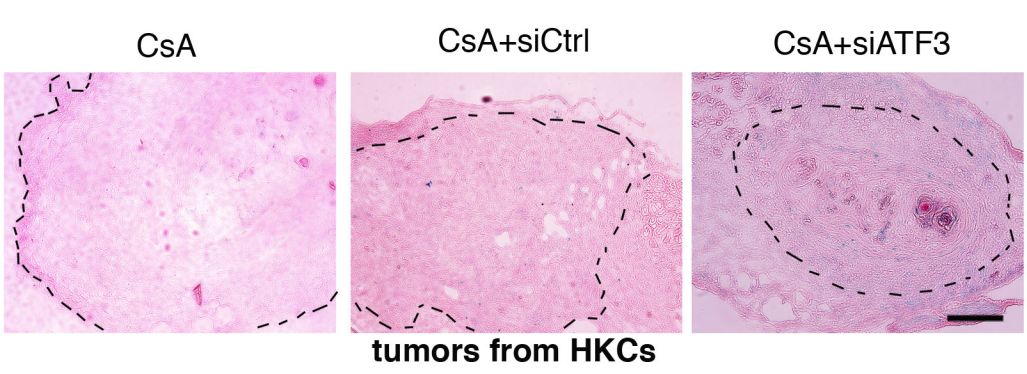

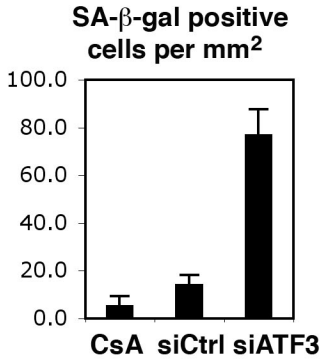

e

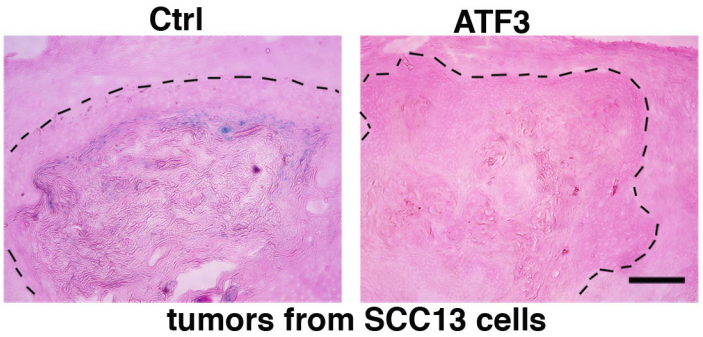

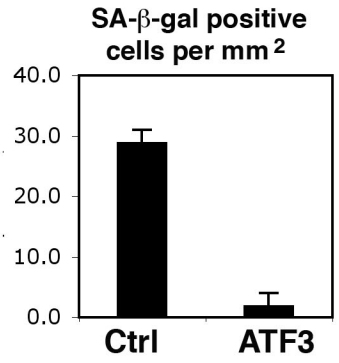

Wu et al_Suppl. Fig. 11

Supplemental Figure 11. Increased ATF3 expression promotes keratinocyte tumour formation and suppresses cancer cell senescence

a, HKCs infected with the ATF3 expressing retrovirus (ATF3) or empty vector control (Ctrl) were subsequently infected with the H- *ras*^{V12} transducing retrovirus. 16 hours after infection, cells were injected subcutaneously at the dermal-epidermal junction of Scid mice. Mice were sacrificed 6 weeks later. The histological results are given as a summary Table, with representative images shown in Fig.3e. **b,** SCC12 and SCC13 cells infected with an ATF3 expressing retrovirus versus empty vector (Ctrl) were injected at the dermal-epidermal junction of immunocompromised (Scid) mice. As summarized in the Table, histological analysis showed that control SCC12 and 13 cells formed highly keratinized cysts, while ATF3 expressing cells produced lesions with histological features of poorly to moderately differentiated SCC. Representative images are shown in Fig. 3f. **c,** HKCs transfected with ATF3-specific and control siRNAs were infected, 24 hours later, with a H-*ras*^{V12} transducing retrovirus followed by injection at the dermal-epidermal junction of Scid mice. Mice were treated every other day with CsA and sacrificed after 10 days. Shown are representative images of histological analysis summarized in Fig. 3g. Bar = 200 μm. **d,** Histological sections of lesions formed in the experiment of the previous panel were analyzed for SA-β-galactosidase activity as in Fig. 3h. Shown are low magnification images as well as quantification of the number of SA-β-gal positive cells. Bar = 100 μm. **e,** Histological sections of lesions formed by SCC13 cells infected with an ATF3 expressing retrovirus versus empty vector control (Ctrl), from the experiment in (b), were stained for SA-β-galactosidase activity. Quantification of number of SA-β-gal positive cells is shown on the right. Bar = 100 μm.

a

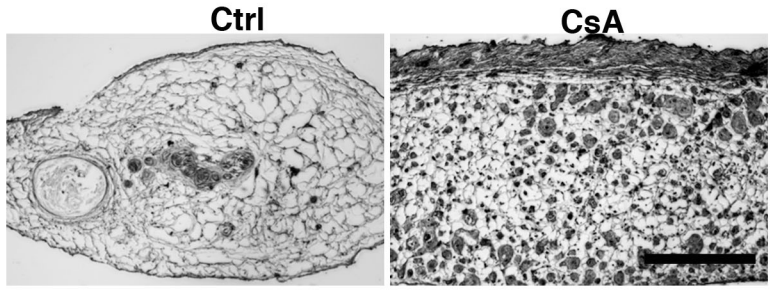

b

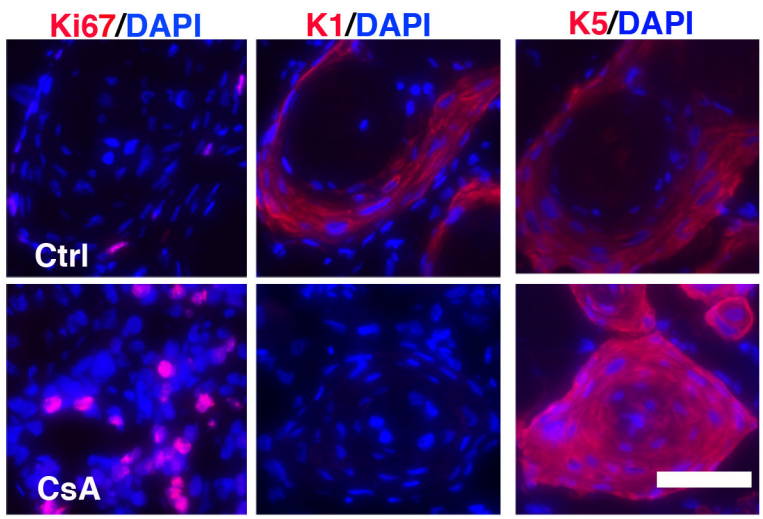

Wu et al_ Suppl. Fig. 12

Supplemental Figure 12. Serial dilution tumourigenicity assays of sorted a6^{bri} CD71^{dim} HKC populations.

a, HKCs were infected with the *Ha-ras^{V12}* expressing retrovirus followed, 20 hrs after infection, by FACS separation of a cell population with high expression of the cell surface markers α6 integrin and low CD71 (α6^{bri}CD71^{dim} cells). Serial dilutions of cells were admixed with a fixed amount of uninfected HKCs (2x10^5 per injection) in matrigel, followed by injection at the dermal-epidermal junction of NOD/SCID interleukin-2 receptor gamma chain null mice. Injected animals were then treated with CsA or ethanol alone, every other day for 4 weeks. Photographs correspond to low magnification images of nodules recovered after injection of low numbers of sorted *Ha-ras^{V12}* expressing HKCs (2,500 per injection), while higher magnification images are shown in Fig. 4a. Quantification of the results after injection of low numbers of *Ha-ras^{V12}* expressing HKCs, as shown in Fig. 4b, was achieved by counting number of proliferative centers (defined as clusters of >40 keratinocytes per center) per mm^2 in 4 nodules per condition, using Nikon NIS Elements measurement software. Quantification of the results after injection of higher numbers of *Ha-ras^{V12}* expressing HKCs, as shown in Fig. 4c, was achieved by histological determination of the number of cysts (defined as mostly keratinized, < 20% solid cell component) and solid tumours (composed >50% by solid cell areas), together with tumour grade. Similar serial dilution tumourigenicity assays were performed, and quantified as indicated in Fig. 4b,c with a sorted α6^{bri}CD71^{dim} population of H-*ras^{V12}*expressing HKCs plus/minus ATF3 overexpression (obtained as for the experiment in Fig. 3e). **b,** Immunofluorescence analysis of nodules recovered after injection of low numbers of sorted *Ha-ras^{V12}* expressing HKCs (2,500 per injection) in mice plus/minus CsA treatment, with antibodies against Ki67 and keratin 1 (K1) as markers of proliferation and differentiation, respectively, and keratin 5 (K5) for keratinocyte

identification. DAPI was utilized for nuclear counterstaining. Images are representative of four independent fields, two samples per conditions. Counting cells in these fields was used also for quantification of the results : keratin-expressing cells in nodules formed in control versus CsA treated animals exhibited 4% versus 20% of Ki67 positivity. Bar=50 μm.

a

quantification of histological lesions

	SCC13+Ctrl			SCC13+ATF3		
No. of cells	cysts	solid tumors	tumor grade	cysts	solid tumors	tumor grade
500	0/4	0/4	-	0/4	2/4	II-III
1000	1/4	0/4	I	0/4	3/4	II-III
2000	2/4	0/4	I	0/4	3/4	III
5000	3/4	1/4	I-II	0/4	4/4	III

b

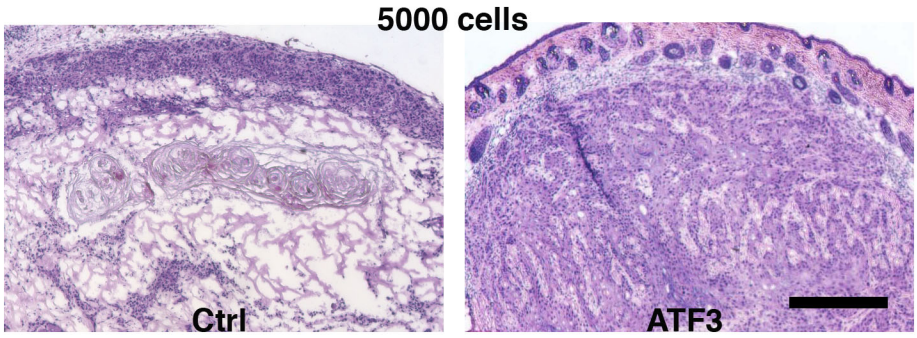

Wu et al_Suppl. Fig.13

Supplemental Figure 13. Increased ATF3 expression enhances tumourigenic potential of sorted SCC sub-populations. a, SCC13 cells infected with the ATF3 expressing retrovirus (ATF3) or empty vector control (Ctrl) were sorted by MAC Beads for CD133 expression. Serial dilutions of CD133+ cells were admixed (in the indicated numbers) with a fixed amount of HKCs ($2x10^5$ cells) prior to injection at the dermal-epidermal junction of Scid mice. To minimize individual animal variations, each mouse received two flank side injections, of control versus ATF3 expressing SCC13 cells. Four mice per cell numbers were injected, and examined for tumour formation 4 weeks later, by macroscopic inspection and histological analysis. The number of cysts (defined as mostly keratinized lesions, < 20% solid cell component) and solid tumours (composed >50% by solid cell areas) are indicated, as well as tumour grade. **b,** Representative histological analysis of tumours formed after injection of 5000 control (Ctrl) or ATF3-expressing CD133+ SCC13 cells. Bar=250μm

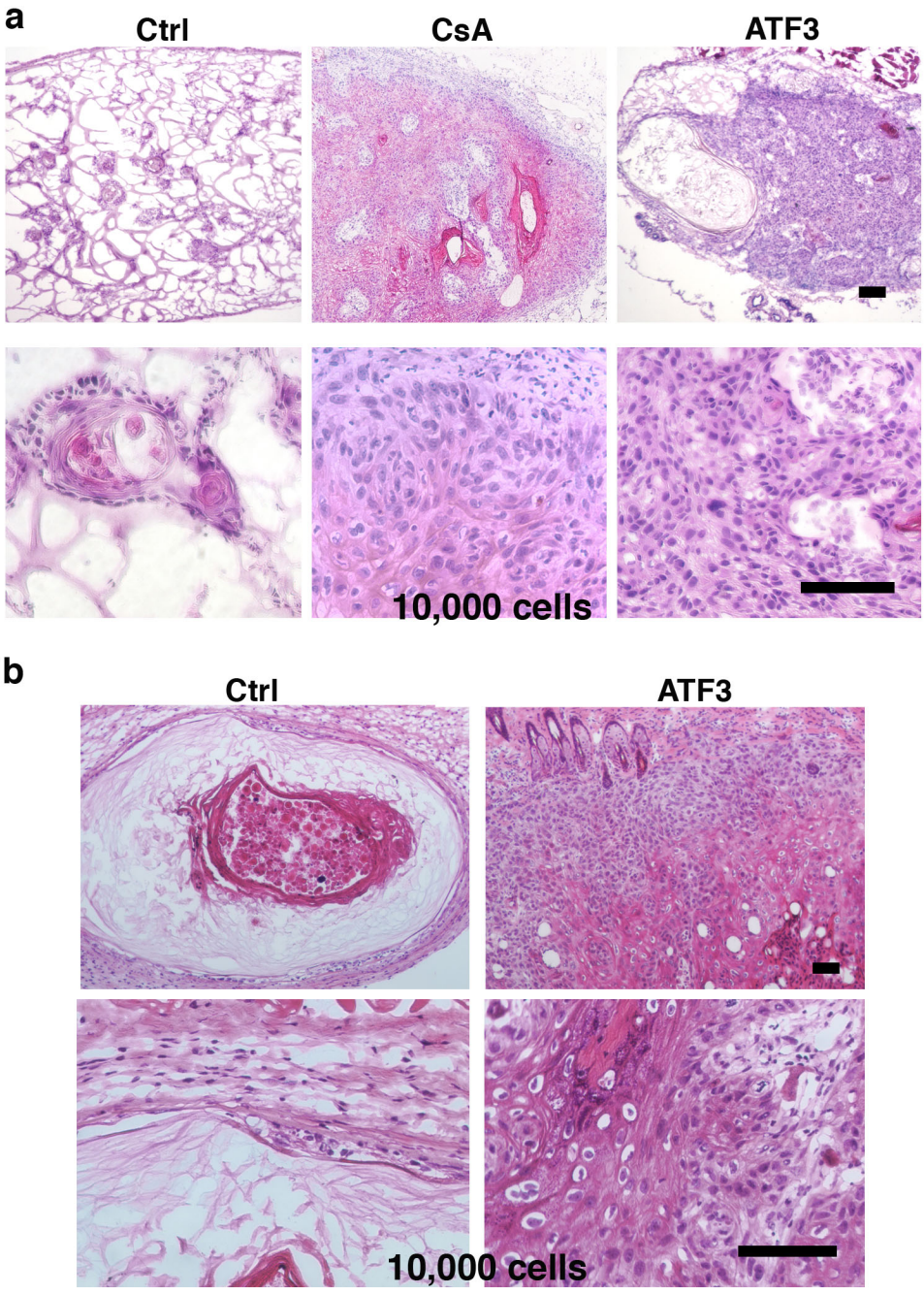

Wu et al _Suppl. Fig. 14

Supplemental Figure 14. Increased ATF3 expression enhances secondary tumour cell growth. a, Primary tumours formed by *Ha-ras*^{V12} expressing HKCs in Scid mice plus/minus CsA treatment were isolated, 6 weeks after cell injection, and dissociated into single cells by collagenase digestion. Serial dilutions of tumour cells were admixed with a fixed amount of HKCs prior to injection at the dermal-epidermal junction of Scid mice, which were also treated with CsA or ethanol control. Similar experiments were performed with freshly dissociated cells from primary tumours formed by *Ha-ras*^{V12} expressing HKCs plus/minus increased ATF3 expression. In all cases, the number of cysts and solid tumours was determined 4 weeks later by macroscopic and histological analysis as summarized in Fig. 4f. Shown are representative images of secondary tumours formed after injection of *Ha-ras*^{V12} expressing HKCs in mice plus/minus CsA treatment or HKCs plus/minus increased ATF3 expression (10,000 cells per injection). **b**, cells from primary tumours formed by control versus ATF3 expressing SCC13 cells were similarly dissociated, serially diluted and utilized for secondary tumour formation assays as in the previous panel. The results are summarized in Fig. 4g. Shown are representative images of secondary tumours formed after injection of 10,000 cells. Bars: 100μm

Supplemental Table I. siRNA sequences used in knock-down experiments.

GENE	siRNA #1	siRNA #2
Calcineurin B1	GCCUGAGUUACAACAGAAUCCUUUA	GGAACAAUCUGAAAGAUACACAGUU
NFATc1	CGAGCCGUCAUUGACUGUGCCGGAA	AGAGAAUUCGGCUUGCACAGGUCCC
ATF3	GGAAAGUGUGAAUGCUGAAdTdT	CGUGCAGUAUCUCAAGAUAdTdT
p53	CCAUCCACUACAACUACAUGUGUAA	CCAGUGGUAAUCUACUGGGACGGAA

Supplemental Table II. Primers (human genes) used in the real time RT-PCR experiments

GENE	FORWARD	REVERSE
36B4	GCAATGTTGCCAGTGTCTGT	GCCTTGACCTTTTCAGCAAG
β–ACTIN	AGAAAATCTGGCACCACACC	GTCTCAAACATGATCTGGG
ATF3	ACGGAGTGCCTGCAGAAAG	TCTCGTTCTTGAGCTCCTCA
p53	TGAGGTTGGCTCTGACTGTA	TTACCACTGGAGTCTTCCAG
c-Jun	GGGAGTGGAGGTGCGCGGAGTCAGG	GAAACACCAGCCCGGGAGCCACAGG
c-Fos	AGACAGCCCGCTCCGTGCCAGAC	CGGGGTAGGTGAAGACGAAGGAAGAC
keratin 1	GTTCCAGCGTGAGGTTTGTT	TAAGGCTGGGACAAATCGAC
p21	CCCAAGCTCTACCTTCCAC	ACAGGTCCACATGGTCTTCC
DcR2	TTGCCTTCTTGCCTGCTATG	TACTGACCTTGACCACCTCT
PAI-1	TGAAGATCGAGGTGAACGAG	GAAAAGGACTGTTCCTGTGG
loricrin	ATGATGCTACCCGAGGTTTG	ACTGGGGTTGGGAGGTAG TT
calcineurin B1	TGAAGATGATGGTGGGGAAC	TTGTGGATATCTAGGCCACC
NFATc1	CAACGGTAACGCCATCTTTC	GACGTCGTTTCTGCGTCTTT
ATF3 promoter Region -3.4kb	TGCATTAGGTGCTATTGTTAGT	GATTGCTAGTTTAATAGTGTCC
ATF3 promoter Region -2.7kb	TACCAAACTGTGACCTTCGG	TGTAGACACAAGTGTGGCCT
ATF3 promoter Region -0.5kb	ACACCACAGACTAACGCTTC	GACTAGGTGAGGCTGGGAA
Calcipressin (RCNA1) promoter NFAT binding region	AGTTGTGCAAACATCACCACA	TTTAGTGGGTGCCAGTGTTTC
β-actin promoter region (no NFAT binding)	TGGTGCGCATCTGTAATCTC	ACCTAGGCTGGAGTGCAGTG

Supplemental Table III: The oligonucleotide sequences for DNA precipitation

Oligio name	FORWARD
p53-1	AAGGAGATTAA**ATAA**GATGGTGTGATATAAAGTATCTGGGAGAAAACGTTAG GGTGTGATA**TTAC**GGAAAGCCTT
mp53-1	AAGGAGATTAA**CGCG**GATGGTGTGATATAAAGTATCTGGGAGAAAACGTTAG GGTGTGATA**GCGA**GGAAAGCCTT
p53-2	AGCACTATTGGTCAAGATGCAGGAAC**CGTCA**GGAGCCCTAGAAACAGGGGAG AGTTAGAAAGCTGG

The underline indicates ATF/CREB binding sites, the bold capital indicating wild-type and substituted core sequence.

Supplementary Notes

1. Lazarov, M., *et al.* CDK4 coexpression with Ras generates malignant human epidermal tumourigenesis. *Nat Med* **8**, 1105-1114 (2002).
2. Zheng, Y., *et al.* Organogenesis from dissociated cells: generation of mature cycling hair follicles from skin-derived cells. *J Invest Dermatol* **124**, 867-876 (2005).
3. Aramburu, J., *et al.* Affinity-driven peptide selection of an NFAT inhibitor more selective than cyclosporin A. *Science* **285**, 2129-2133 (1999).
4. Kolev, V., *et al.* EGFR signalling as a negative regulator of Notch1 gene transcription and function in proliferating keratinocytes and cancer. *Nat Cell Biol* **10**, 902-911 (2008).
5. Dimri, G.P., *et al.* A biomarker that identifies senescent human cells in culture and in aging skin in vivo. *Proc Natl Acad Sci U S A* **92**, 9363-9367 (1995).
6. Neal, J.W. & Clipstone, N.A. A constitutively active NFATc1 mutant induces a transformed phenotype in 3T3-L1 fibroblasts. *J Biol Chem* **278**, 17246-17254 (2003).